Fundamental Interactions of Molecules (Na$_2$, Na$_3$) with Intense Femtosecond Laser Pulses

THOMAS BAUMERT* AND GUSTAV GERBER

Fakultät für Physik, Universität Freiburg, D-79104 Freiburg, Germany

Abstract. The real-time dynamics of multiphoton ionization and fragmentation of molecules Na$_2$ and Na$_3$ has been studied in molecular beam experiments employing ion and electron spectroscopy together with femtosecond pump-probe techniques. Experiments with Na$_2$ and Na$_3$ reveal unexpected features of the dynamics of the absorption of several photons as seen in the one- and three-dimensional vibrational wave packet motion in different potential surfaces and in high laser fields:

In Na$_2$ a second major resonance-enhanced multiphoton ionization (REMPI) process is observed, involving the excitation of two electrons and subsequent electronic autoionization. The possibility of controlling a reaction by controlling the duration of propagation of a wave packet on an electronically-excited surface is demonstrated. In high laser fields, the contributions from direct photoionization and from the second REMPI process to the total ion yield change, due to different populations in the electronic states participating in the multiphoton ionization (MPI) processes. In addition, a vibrational wave packet motion in the electronic ground state is induced through stimulated emission pumping by the pump laser. The $4\,^1\Sigma_g^+$ shelf state of Na$_2$ is given as an example for performing frequency spectroscopy of high-lying electronic states in the time domain. Pure wave packet effects, such as the spreading and the revival of a vibrational wave packet, are investigated.

The three-dimensional wave packet motion in the Na$_3$ reflects the normal modes in the X and B states, and shows in addition the pseudorotational motion in the B state in real time.

I. INTRODUCTION

Multiphoton ionization (MPI) of small molecules has been studied in recent years by a variety of techniques, and is generally well understood. The ionization is predominantly due to resonance-enhanced multiphoton (REMPI) processes, whereas nonresonant multiphoton processes only play a minor role. Until now, there have been few studies of the dynamical aspects of the interaction of laser radiation with molecules and details of the excitation processes and the different decay channels of highly excited states, embedded in the ionization and in the fragmentation continuum. Recently we reported on the interaction of a bound doubly-excited molecular state with different continua, and the competition between the various decay channels.[1] In that study, we used femtosecond laser pulses as an experimental tool to distinguish between the dissociative ionization of the molecule and the neutral fragmentation with subsequent excited-fragment photoionization. Both processes are difficult to distinguish when using nanosecond or even picosecond laser pulses. This distinction is of particular importance in

multiphoton ionization studies of metal cluster systems.[2] The multiphoton ionization and fragmentation of alkali-metal molecules and, in particular, of Na$_2$ and Na$_3$, has attracted considerable interest. In many experiments with Na$_2$ it has been found that, in conjunction with the formation of Na$_2^+$ ions, ionic fragments Na$^+$ are also formed. REMPI processes via the A$^1\Sigma_u^+$ or the B^{1}P$_u$ states are responsible for this observation.[3] The sodium trimer Na$_3$ is probably the most studied and best known small metal-cluster.[4] Its excitation spectrum consists of several bands due to different excited electronic states, among which the B-state, with an onset at 625 nm, is of greatest interest. This is because of the observed pseudorotational features in the spectra. In a series of beautiful experiments, Khundkar and Zewail[5] have demonstrated the enormous advantage of applying femtosecond lasers to the study of molecular dynamics. Their pioneering work in the field of femtosecond photochemistry and transient molecular fluorescence spectroscopy has initiated other time-resolved ultrafast laser studies.[6]

*Author to whom correspondence should be addressed.

Time-resolved measurements often open up new directions and provide a more comprehensive view of the physical and chemical processes. Due to recent developments in the generation and amplification of ultra-short light pulses, direct measurements of transient ionization and fragmentation spectra with femtosecond time resolution are now possible. This allows a closer look at the dynamical aspects of multiphoton ionization and fragmentation of molecules and clusters (for recent time-resolved cluster work, see, for example, ref 7).

In this paper we discuss experimental results of time-resolved studies of multiphoton ionization and fragmentation processes of sodium molecules in molecular beam experiments applying femtosecond pump-probe techniques and ion and electron spectroscopy.

After describing our experimental setup in section II, we present and discuss our results in section III. That part starts with the two different MPI processes which we have observed in our femtosecond pump-probe studies on Na_2. Several aspects of these experiments are highlighted next: the possibility of controlling reactions, high laser field effects, the observation of a ground state wave packet, and the possibility of performing spectroscopy in the time domain. Before we summarize in part IV, we depict the long time behavior of a one-dimensional vibrational wave packet, and outline the three-dimensional wave packet motion on the bound potential energy surfaces of the X and B states in Na_3.

II. EXPERIMENT

In our femtosecond laser-molecular/cluster beam studies of time-resolved multiphoton ionization and fragmentation processes, we employ a combination of different experimental techniques. Femtosecond pump-probe techniques are used to induce and to probe molecular/cluster transitions, to resolve the interactions, and to display the evolution of coherences and populations in real-time. A supersonic beam provides the molecules in a collision-free environment and restricts the initial states to the very lowest vibrational and rotational states. Time-of-Flight (TOF) spectroscopy is used to analyze the final continuum states by measuring the released kinetic energy of the ionic fragments and the energy distribution of the ejected electrons. Figure 1 shows the schematic experimental arrangement of the molecular beam, the femtosecond laser pulses, and the ion and electron TOF spectrometers. The supersonic beam is produced either by a pure sodium expansion through a small orifice of typically 0.15 mm diameter, or by an expansion seeded with argon. The oven is usually operated at 1000 K with nozzle temperatures about 50 K higher.

Femtosecond light pulses are generated in two different home-built laser systems. Independently tunable femtosecond pulses down to 50 fs time duration and up to 50 μJ energy are generated in the laser system shown in Fig. 2. The tunability of our present system covers the near UV, the complete visible range, and the near IR. The output pulses of a colliding-pulse
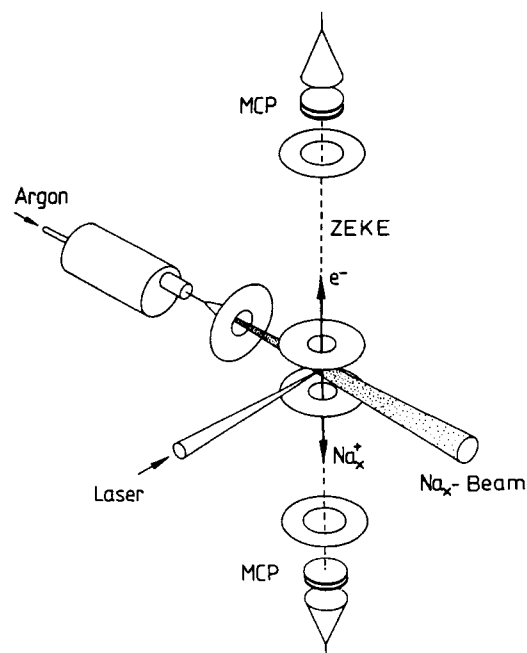

Fig. 1. Schematic experimental setup. Pump and probe laser beams are collinear and perpendicular to the molecular beam and the TOF spectrometers.

mode-locked ring dye laser (CPM) are amplified in a bow-tie amplifier, which is pumped by an excimer laser at 308 nm, pulse compressed, and focused into a cell containing methanol to generate a white light continuum. Pump and probe pulses at specific wavelengths are selected from the white light continuum in a grating arrangement, which can also be used to compensate for group velocity dispersion in the subsequent amplification stages. Using adjustable slits for wavelength selection, the bandwidth of the pulses can be chosen depending upon the requirements of the experiment. Pump and probe pulses are amplified again in two additional bow tie amplifiers. If desired, additional wavelength conversion methods like frequency doubling are used, before recombining pump and probe beams collinearly and focusing them into the interaction region. A Michelson arrangement is used to delay the probe laser relative to the pump laser. The ultimate phase-sensitive time resolution obtained with such a setup is about 1 fs, as illustrated by the interferometric autocorrelation shown in Fig. 3.

The second femtosecond laser system makes use of a home-built Ti:Sapphire laser oscillator. This Ti:Sapphire laser produces light pulses of 20–70 fs time duration in the wavelength range of 700–850 nm. Again using a bow-tie amplifier, pulse energies of the order of several tens of microjoules are obtained.

Most of the experiments described in this contribution were performed with identical pump and probe pulses extracted from the amplified fundamental of the CPM laser around 2 eV. This has the advantage of a precise zero delay time determination, which, for example, is useful for measuring phase shifts with respect to time zero. Moreover, since many nanosecond laser REMPI experiments are done with one color, the additional new information extracted from time domain experiments is directly

related to the nanosecond REMPI work using identical femtosecond pump and probe laser pulses.
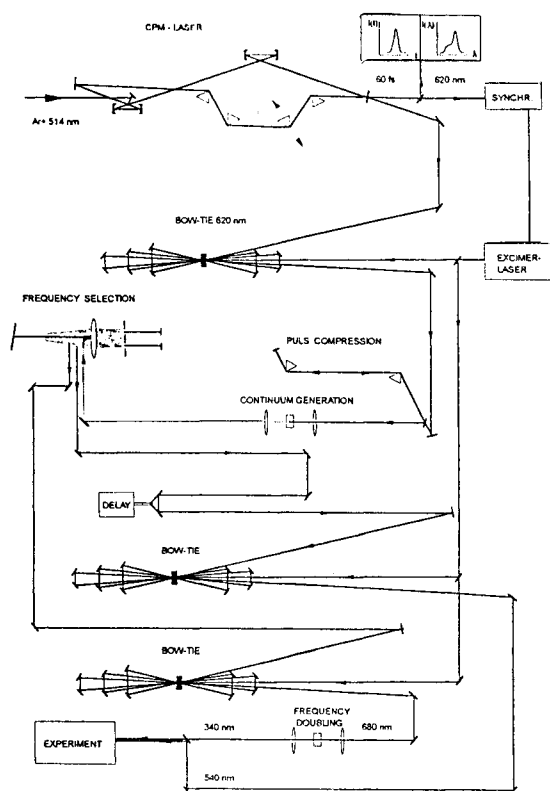

Fig. 2. Femtosecond laser system for independently tunable pump and probe wavelengths.
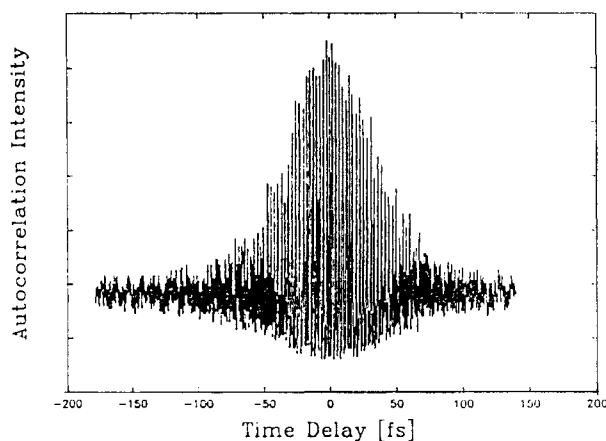

Time Delay [fs]

Fig. 3. Interferometric autocorrelation of a Ti:Sapphire pulse at 773 nm having a pulse duration of 40 fs $sech^2$. The figure displays the ultimate phase-sensitive time resolution of our setup, being in the order of 1 fs.

III. RESULTS AND DISCUSSION

A) Na_2 — MPI Processes

We have recently reported femtosecond time-resolved multiphoton ionization and fragmentation dynamics of the Na_2 molecule. From the real-time observation of vibrational wave packet motions, it was concluded that two different physical processes determine the time evolution of multiphoton ionization.[8] The observed femtosecond pump-probe delay spectrum of the molecular ion (Na_2^+) signal is shown in the upper part of Fig. 4. It is evident from the beat structure seen in this transient that there are two frequencies involved. Therefore, there are two contributions to the transient ionization spectrum. The envelope intensity variation reveals them to be 180° out of phase. A Fourier analysis of this spectrum yields two groups of frequencies, one centered at 108.1 cm^{-1} and a second centered at 92.2 cm^{-1}, with an experimental uncertainty of less than 0.5 cm^{-1}. From the observed two oscillation periods, the 180° phase shift and the additionally measured time-resolved Na^+ photo-fragmentation spectrum (see lower part of Fig. 4), we concluded that for Na_2, two different multiphoton ionization processes exist that require incoherent addition of the intensities to account for the observations. If these two contributions to the observed oscillating Na_2^+ signal would have been just two different intramolecular ionization pathways leading to the same indistinguishable final states, the amplitudes
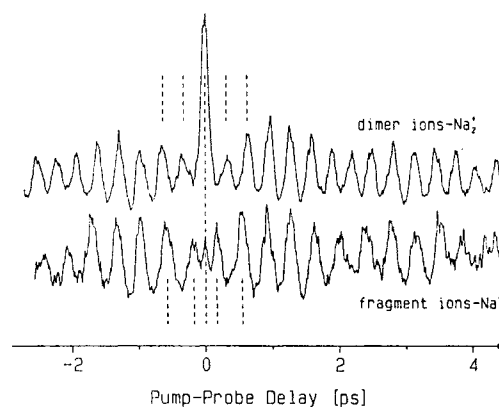

Pump-Probe Delay [ps]

Fig. 4. *Upper part*: transient Na_2^+ signal obtained as a function of pump-probe delay time between two identical femtosecond laser pulses with 85 fs at $\lambda_{max}= 623$ nm. The envelope intensity variation and the oscillatory structure of this transient Na_2^+ MPI signal reveal two contributions out of phase by 180°. They correspond to independent wave packet motions in bound molecular potentials with 309 fs ($A\ ^1\Sigma_u^+$) and 362 fs ($2\ ^1\Pi_g$) oscillation period. *Lower part*: transient Na^+ fragment signal, obtained under the same experimental conditions as the Na_2^+ transient. The transient shows the dynamics of the 180° phase shifted $2\ ^1\Pi_g$ state wave packet motion.

Baumert and Gerber / Femtosecond Dynamics of Molecules

for ionizing out of the A $^1\Sigma_u^+$ state and out of the 2 $^1\Pi_g$ state should be added coherently. The coherent addition would lead to a different total Na_2^+ signal, as direct ionization out of the 2 $^1\Pi_g$ state leads to a time-independent signal.[10, 20] Moreover, the two different MPI processes result in two different sets of final vibrational levels.

The direct photoionization of an excited electron, where one pump photon creates a vibrational wave packet in the A $^1\Sigma_u^+$ state and two probe photons transfer that motion via the 2 $^1\Pi_g$ state in the ionization continuum, is one (REMPI) process. Figure 5 shows this *one electron* direct photoionization process. As all three photons are absorbed at the inner turning point, this is an MPI process where all photons could be absorbed at once, or at least within the time duration of the light pulses.

The second involves excitation of *two electrons* and subsequent electronic autoionization. Here two pump photons create a wave packet at the inner turning point, in the 2 $^1\Pi_g$ Rydberg state, which then propagates to the outer turning point, where the probe laser transfers the

motion into the continuum by exciting a second electron, forming a doubly-excited neutral Na_2^{**} molecule. This happens only at the outer turning point of the 2 $^1\Pi_g$ state periodically after each round trip. In this case, the probe photon is absorbed, at the earliest, about 180 fs after the pump photons were absorbed. Figure 6 illustrates the two-photon-pump and one-photon-probe ionization process which involves excitation and decay of doubly-excited states. The decay of these doubly-excited states takes place by electronic autoionization into the $^2\Sigma_g^+$ ground state of Na_2^+, being responsible for the observed 180° phase-shifted 2 $^1\Pi_g$ wave packet motion in the Na_2^+ transient (upper part of Fig. 4), and by electronic autoionization-induced fragmentation leading to slow Na^+ atomic fragments. This interpretation is confirmed by the observed 180° phase-shifted 2 $^1\Pi_g$ state wave packet dynamics seen in the Na^+ ionic fragment transient displayed in the lower part of Fig. 4.

Recent preliminary calculations of doubly-excited neutral electronic states of Na_2 correlating with the $Na(4s)$
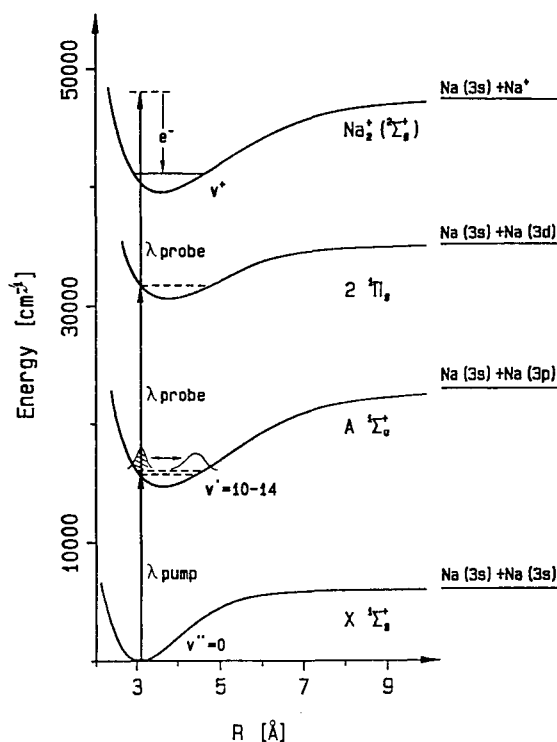

Fig. 5. Scheme for a one-photon pump and two-photon probe direct ionization. The potential energy curves for the involved electronic states are shown. The pump pulse prepares a coherent superposition of the vibrational states $v'=10-14$ in the electronic A $^1\Sigma_u^+$ state at the inner turning point for a 70 fs pulse at a center wavelength of 627 nm. The motion of the vibrational wave packet is probed by a time-delayed fs laser pulse in a two-photon probe process into the ionization continuum via the 2 $^1\Pi_g$ state.
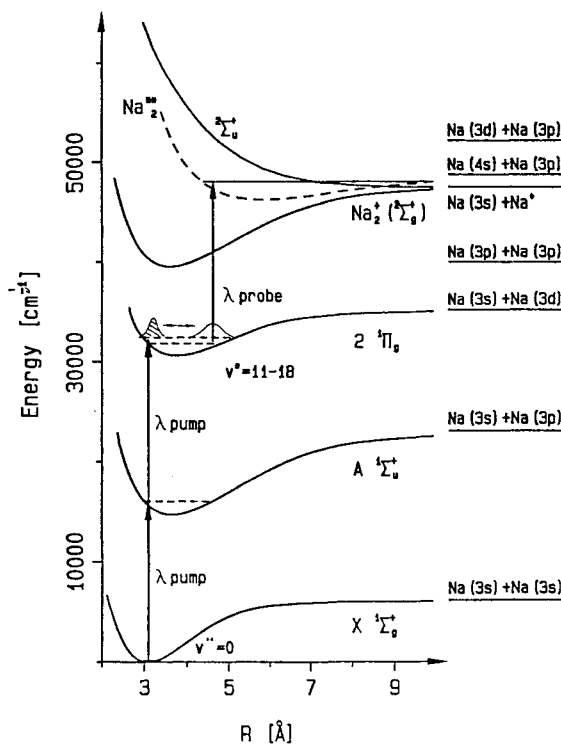
Fig. 6. Ionization scheme for a two-photon-pump transition to the electronic 2 $^1\Pi_g$ state, and an indirect one-photon ionization which proceeds via excitation of a bound doubly-excited state of Na_2 and subsequent electronic autoionization. The dashed line is an estimate for the potential curve of Na_2^{**}. Recent calculations of doubly-excited states are shown in Fig. 7. The probe process occurs only at the outer turning point, explaining the 180° phase shift of the 2 $^1\Pi_g$ wave packet motion in Fig. 4.

+ Na(3p) asymptote performed by Meyer[9] show a $^1\Pi_u$ state that can be excited from the outer turning point of the 2 $^1\Pi_g$ state by absorption of a one-probe photon, as indicated in Fig. 7. Although this state can decay by electronic autoionization, it cannot decay by electronic autoionization-induced fragmentation. This is why there has to be a spin orbit interaction with the nearby $^3\Pi_u$ doubly-excited state via which the fragmentation proceeds.

We performed these experiments with the center wavelengths of our lasers from 618 nm up to 627 nm, and pulse durations from 70 fs up to 110 fs. For low excitation intensities, no change in the global behavior of the measured transients was observed. Only the oscillation periods of the A $^1\Sigma_u^+$ state wave packet and of the 2 $^1\Pi_g$ state wave packet show slight variations according to the different spectral regions excited.

The Na_2 case is the first example of a femtosecond molecular multiphoton ionization study. It was only through time domain measurements that the existence of a second major ionization process was established. A comprehensive discussion based on classical arguments can be found in ref 10, whereas a comparison between experiment and quantum mechanical calculations can be found in ref 11.
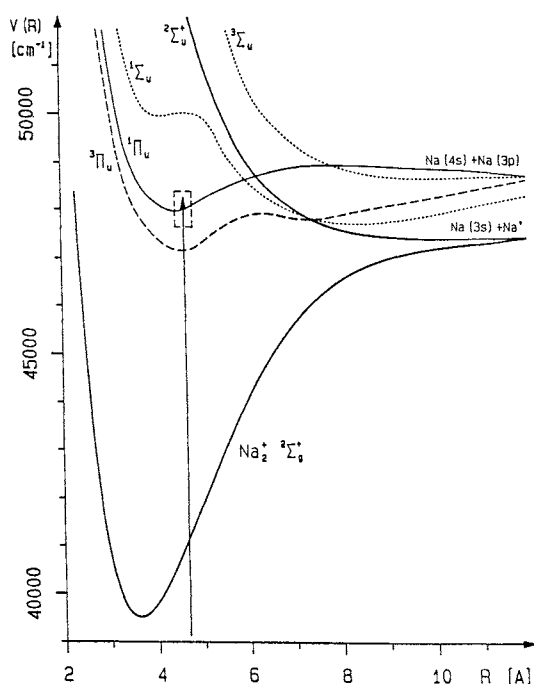
Fig. 7. The potential energy curves of the $^2\Sigma_g^+$ and $^2\Sigma_u^+$ states of Na_2^+ and four doubly-excited neutral states of Na_2 are shown. These curves are drawn on the basis of unpublished calculations by Meyer.[9] The excitation of the $^1\Pi_u$ doubly-excited state by absorption of one-probe photon at the outer turning point of the 2 $^1\Pi_g$ state is indicated.

B) Na_2 — Control of Na_2^+ versus Na^+ Production

Controlling a chemical reaction so that a given product is produced at the expense of another, energetically-allowed, product is one of the basic issues in physical chemistry. Many publications are devoted to this topic. Some references can be found in a recent review by Warren et al.[12] Since in larger molecules the locally-deposited energy redistributes very rapidly throughout the molecule, specially designed pulse shapes and phase-shifted pulses are currently discussed to be used in order to achieve bond selectivity in these systems. For smaller molecular systems, however, the basic ideas of the Tannor–Kosloff–Rice[13] scheme are applicable. They have proposed that controlling the duration of propagation of a wave packet on an excited electronic potential energy surface, by simply controlling the time delay between pump and probe pulses, can be used to generate different chemical products on the ground state potential energy surface. This idea of controlling the duration of propagation of a wave packet on an excited electronic surface was realized in an experiment by Zewail and coworkers.[14] They used two sequential coherent laser pulses to control the reaction of I_2 molecules with Xe atoms to form XeI. It was shown that the yield of product XeI is modulated as the delay between the pulses is varied, reflecting its dependence on the nuclear motions of the reactants. However, an example how the propagation of wave packets can be used to produce one product at the expense of another energetically-allowed product is given by our experiments for the first time, to our knowledge.

In order to make the topic more clear, let us assume that we focus a nanosecond laser on our molecular beam having a photon energy of about 2 eV. After absorption of three photons, we will detect Na_2^+ and Na^+ in our TOF spectrometers according to the two ionization processes described before. There are no simple means to produce Na_2^+ at the expense of Na^+ with this nanosecond laser at a fixed intensity and wavelength. Using the time-resolved approach, we know that at the inner turning point of the A $^1\Sigma_u^+$ and 2 $^1\Pi_g$ states in Na_2, the molecule is directly ionized by the probe laser (see Fig. 5), whereas only at the outer turning point of the 2 $^1\Pi_g$ state are fragment Na^+ ions produced by exciting the doubly-excited state with its subsequent decay channels (Fig. 6). Thus, by controlling the duration of propagation of the wave packets on the A $^1\Sigma_u^+$ and 2 $^1\Pi_g$ states in Na_2, we are able to produce Na_2^+ at the expense of Na^+ by adjusting the pump-probe delay time. This is illustrated in Fig. 8, where we display the ratio of the Na_2^+ signal over the Na^+ signal from Fig. 4. A modulation of this ratio of at least a factor of two is seen as a function of pump-probe delay.
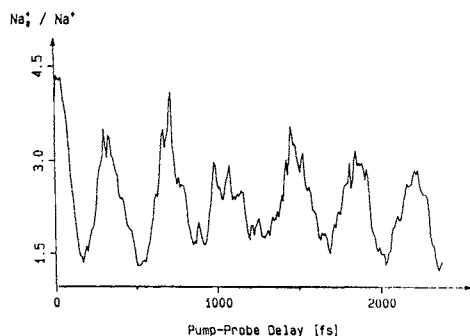
Fig. 8. Controlling the Na_2^+ production versus the Na^+ production in a Tannor–Kosloff–Rice-like scheme by adjusting the pump-probe delay time and therefore controlling the internuclear distance of the molecule.

C) Na_2 — High Laser Field Effects, Ground State Wave Packet

In a further study, the dependence of the total Na_2^+ ion signal on the intensity of the femtosecond pulses was investigated in detail.[15] The experimental results, shown in the upper part of Fig. 9, were obtained for three different intensities ($I_0=10^{12}$ W/cm^2, $0.3*I_0$, and $0.1*I_0$). The curves exhibit periodic oscillations with different periods for different laser intensities. The periodic contributions to these transients were analyzed by taking their Fourier transform, displayed in the lower part of Fig. 9. For higher laser intensities, the relative contributions from the A $^1\Sigma_u^+$ and the 2 $^1\Pi_g$ states change dramatically, indicating the increasing importance of the two-electron versus the one-electron process. For the strongest fields used in these experiments, a vibrational wave packet motion in the electronic ground state X $^1\Sigma_g^+$ is observed. It is created through stimulated emission during the time the ultrashort pump pulse interacts with the molecule. This ground state wave packet dynamic is monitored by absorption of three photons from the time-delayed probe laser in a direct photoionization process.

Time-dependent quantum calculations were performed to explain this behavior. They show that for different laser field strengths, the electronic states involved in the MPI and coupled coherently by the laser interaction, are populated differently in a Rabi-type process. For lower intensities, the A $^1\Sigma_u^+$ state is preferentially populated by the pump pulse and the A $^1\Sigma_u^+$ wave packet motion dominates the ion signal. For the highest intensity used in these experiments, the contribution of the 2 $^1\Pi_g$ state motion dominates. The reason for this is that after the pump pulse is over, the 2 $^1\Pi_g$ state is populated more than the A $^1\Sigma_u^+$ state. The population in the A $^1\Sigma_u^+$ state is initially increasing with the rising part of the pump pulse, but then the Rabi-type process starts to decrease the population again.
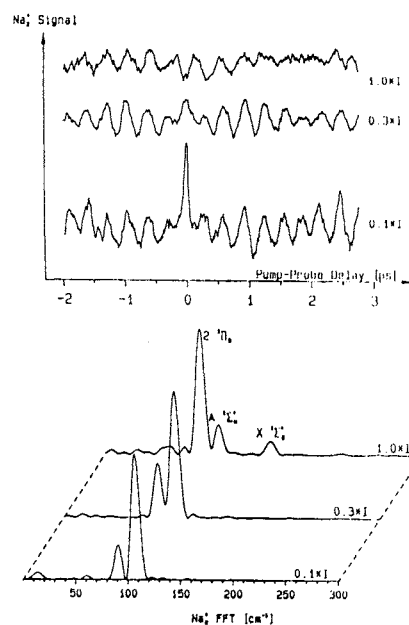

Fig. 9. The upper part of the figure shows transient Na_2^+ spectra as a function of delay time between pump and probe pulses. Different intensities were used as indicated. Below, the Fourier transforms of the transient spectra are displayed. Note the dramatic change of the Fourier amplitudes as a function of intensity. At 1.0 × I, a contribution of the X $^1\Sigma_g^+$ ground state wave packet to the transient ionization spectrum is observed in the Fourier spectrum.

This behavior is nicely illustrated in Fig. 10 for four different laser intensities (for computational details see refs 15, 16). Thus, by changing the intensity of the laser, one may selectively control the relative strength of the direct one-electron photoionization versus the two-electron excitation and electronic autoionization process. This intensity-dependent effect will be used in future experiments to optimize the control scheme of part B.

D) Na_2 — Time-Resolved Spectroscopy of High-Lying Electronic States

We have shown in the last section that by increasing the laser intensity and observing intensity-dependent changes in the transients, we obtain well defined access to higher-lying electronic states in a multiphoton excitation scheme. In this section we will give an example of frequency spectroscopy of a high-lying electronic state, excited by two photons, in the time domain. The spectroscopic information can be derived from data taken in the time domain by a Fourier transformation. This has been shown for diatomics and diatomic-like molecules by Zewail's group for the systems I_2[17] and ICN.[18] Although the time-resolved approach cannot compete with the elaborate techniques of high-resolution spectroscopy for
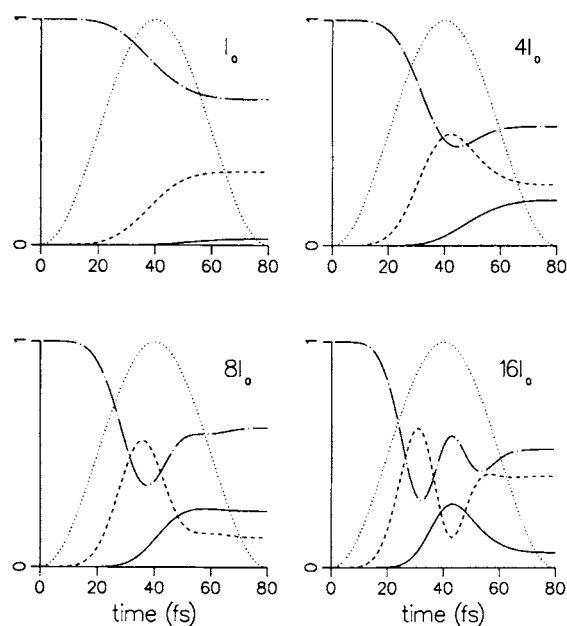
Fig. 10. The electronic states involved in the MPI processes and coupled coherently by the laser interaction are populated differently in a Rabi-type process: the figure shows the change of population in the $X\ ^1\Sigma_g^+$ (dash-dot line), $A\ ^1\Sigma_u^+$ (dash-dash line), and $2\ ^1\Pi_g$ (solid line) states of Na_2 during the pump pulse (dot-dot line) interaction for four intensities.[16] The creation of a ground state $(X\ ^1\Sigma_g^+)$ wave packet by stimulated emission pumping at higher intensities is seen, as well as the observed change of the final population of the $A\ ^1\Sigma_u^+$ and $2\ ^1\Pi_g$ states $(I_0, 4I_0,$ and $8I_0)$. Calculated transients[15] are in agreement with the measured transients displayed in Fig. 9. For the highest intensity $(16I_0)$, the Rabi-type process is clearly seen.

bound systems, for predissociating or dissociative systems this approach might sometimes be the only choice in order to determine spectroscopic data, especially in the transition state region. Another advantage of the time-resolved method is the ease of distinction between vibrational and rotational spectroscopic information, because their energy spacings (e.g., oscillation periods) are different by two orders of magnitude. For bound systems the achievable resolution is only limited by the scan length. Using a square window in the Fourier transformation, the theoretical resolution limit is, for example, $1\ cm^{-1}$ for a scan length of 30 ps.

After absorption of two-pump photons centered at 618 nm, the $4\ ^1\Sigma_g^+$ state of the sodium dimer is excited around the shelf region at the inner turning point. This state, spectroscopically determined by Stwalley and coworkers,[19] is displayed together with the $2\ ^1\Pi_g$ state in Fig. 11. Direct ionization out of this state would result in a time-independent Na_2^+ signal. The same result is obtained in theoretical studies of direct photoionization out of
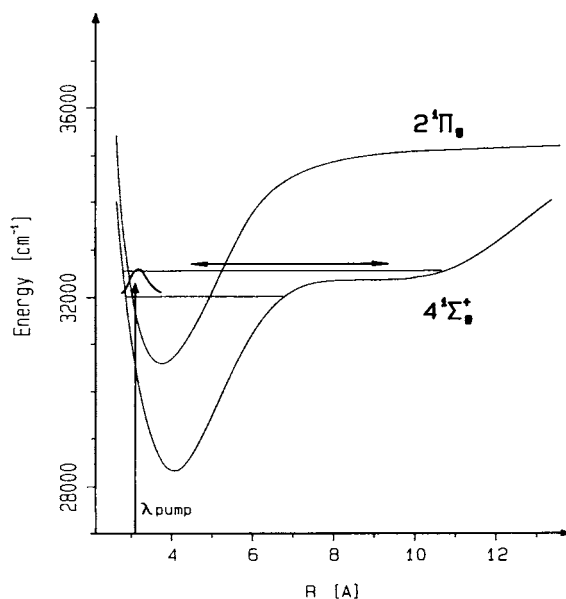

Fig. 11. Excitation of a vibrational wave packet in the $4\ ^1\Sigma_g^+$ state and in the $2\ ^1\Pi_g$ state of Na_2 at the inner turning point by absorption of two photons at $\lambda_{max}= 618$ nm and 110 fs time duration. The two horizontal bars indicate the spectral width of the fs laser pulses, showing that the wave packet propagates in the shelf region of the $4\ ^1\Sigma_g^+$ state.

the $2\ ^1\Pi_g$ state.[20] To explain the observed features, we suggest that, on the one hand, in the probe transition the excitation of a doubly-excited neutral state of Na_2 is again involved, and on the other hand, a stimulated emission process due to the probe laser interaction at the inner turning point takes place and thus introduces a time dependence in the transient ionization signal. Although we did not unambiguously detect the partial reflection of a wave packet at a potential step in our time-resolved experiments, we were able to resolve the vibrational spacings close to the shelf region by taking the Fourier transformation of our data. The results, displayed in Fig. 12 on a logarithmic scale, show the high-intensity behavior discussed before: The transient is dominated by the contributions of the wave packet propagating in the $2\ ^1\Pi_g$ state, whereas the contributions of the $X\ ^1\Sigma_g^+$ ground state and of the $A\ ^1\Sigma_u^+$ state wave packet are comparable. The observed group of frequencies up to $50\ cm^{-1}$ is assigned to the $4\ ^1\Sigma_g^+$ shelf state, using the high-resolution data (see Table 1).

E) Na_2 — Spreading and Recurrence of a Vibrational Wave Packet

At low laser intensities, the Na_2^+ transient is dominated by the oscillating contribution of the $A\ ^1\Sigma_u^+$ state wave packet motion due to the direct photoionization process described before (see part III A and C and Fig. 5). Using

Table 1. ΔG_v values obtained by Fourier transformation of femtosecond time domain data on a Na_2^+ transient (see Fig. 12) in comparison to high-resolution results

v^* (4 $^1\Sigma_g^+$)		ΔG_v Stwalley et al. [cm^{-1}]	ΔG_v from fs work [cm^{-1}]
45	46	48.56	47.5
46	47	45.20	47.5
47	48	41.48	not resolved
48	49	37.00	36.8
49	50	30.80	31.2 (weak)
50	51	22.42	22.4
51	52	8.21	6.5

At $v^* = 51,52$, the 4 $^1\Sigma_g^+$ potential of Na_2, displayed in Fig. 11, widens. At FWHM of our fs laser pulse at a center wavelength of 618 nm we excite the levels $v^* = 47–65$ in this state; whereas at 90% of the spectral distribution, $v^* = 44–76$ are accessible. From $v^* = 52$ to $v^* = 65$, the vibrational spacing is increasing monotonically from 10.5 cm^{-1} to 18 cm^{-1}. In this energy range, only a small Fourier component around 14 cm^{-1} is observed. It is not understood why the part of the wave packet above the shelf is not detected, whereas contributions to the wave packet below the shelf are seen.

the femtosecond pump-probe technique, we are therefore able to study the long-time behavior of a vibrational wave packet. The spreading and recurrence of the vibrational wave packet in the bound A $^1\Sigma_u^+$ electronic state is such a long-time behavior and has been studied in pump-probe experiments. Time-dependent quantum calculations reproduce the measured effects.[21] The spreading and recurrence is basically given by the anharmonicity of a real diatomic molecular potential: there the energy splitting $\Delta(v+1, v) = E_{v+1} - E_v$ varies as a function of v. Thus, the classical oscillation periods $T(v+1, v) = h/\Delta(v+1, v)$ will change, as well, with the vibrational quantum number v. For three vibrational levels and the assumption that $T(v+1, v) > T(v, v-1)$, the phase of the wave function will resemble the one for time $t = 0$ if $kT(v+1, v) = (k+1)T(v, v-1)$, where k counts the number of periods which have passed. This defines the recurrence time (for a more general discussion see ref 22):

$$T_{rec} = \frac{T(v + 1, v) \, T(v, v-1)}{T(v + 1, v) - T(v, v-1)}$$

Taking the known spectroscopic constants of the A $^1\Sigma_u^+$ state[23] into account, we can calculate a recurrence time of 47 ps for laser pulses of 618 nm central wavelength and a temporal width of 65 fs. In Fig. 13, snapshots of the measured and calculated wave packet dynamics in the A $^1\Sigma_u^+$ state for three different times (2 ps, 30 ps, 46 ps) are shown. At early times around 2 ps, the vibrational wave packet nicely illustrates the classical motion of the two nuclei. After 30 ps, the wave packet is
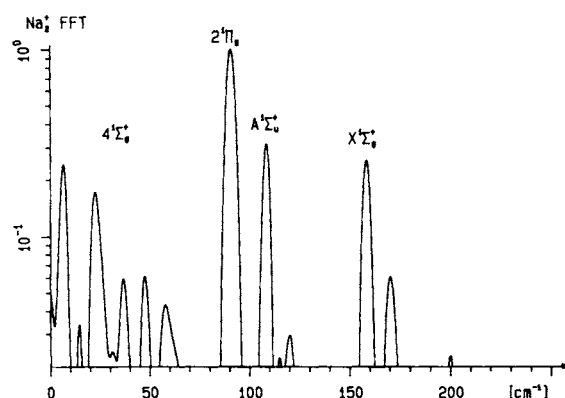

Fig.12. Fast Fourier transform spectrum of a Na_2^+ transient recorded with intense identical pump-probe pulses at $\lambda_{max} = 618$ nm. The contributions of wave packet motion in the X $^1\Sigma_g^+$, A $^1\Sigma_u^+$, 2 $^1\Pi_g$, and 4 $^1\Sigma_g^+$ potential curves to the transient Na_2^+ signal are seen. The ground state wave packet (X) is created by stimulated emission pumping during the pump pulse duration. The A-state wave packet is formed by the absorption of one photon, whereas the last two states are excited by a two-photon absorption. The individual vibrational energy differences contained in the wave packet formed in the shelf region of the 4 $^1\Sigma_g^+$ state are resolved (see Table 1).

completely dispersed and fills the entire classically-allowed region. At any instant of time, one finds a probability density at the inner potential region where the transition to the ion takes place. Consequently, the ion signal has lost its periodic intensity variation. After 47 ps, however, the wave packet is localized as it is for short times, and again it moves periodically back and forth in the bound state potential.

Theoretical investigations of the dynamics of atomic Rydberg wave packets showed "fractional revivals"[24] that have recently been seen in Rydberg wave packet experiments on Rb.[25] They occur at fractions of the revival time when the wave packet has split into two or more separate parts. These effects have not yet been seen in vibrational wave packet studies, including the present A $^1\Sigma_u^+$ experiments. The smaller the vibrational spacings, the longer the oscillation periods. Therefore, with a given temporal resolution, the "fractional revivals" are expected to be observed much more easily under these circumstances. This is why we are currently studying the wave packet dynamics in the 2 $^1\Sigma_u^+$ double-minimum state of Na_2.[26] The principle idea of this experiment is sketched in Fig. 14. A pump pulse at 341 nm prepares a wave packet at the inner turning point of the 2 $^1\Sigma_u^+$ state above the barrier. The probe laser is tuned to 547 nm in order to transfer the wave packet onto $^2\Sigma_u^+$, the repulsive ionic curve only at the outer turning point of the double-minimum state. This experiment requires all parts of the femtosecond laser system shown in Fig. 2. In Fig. 15 the
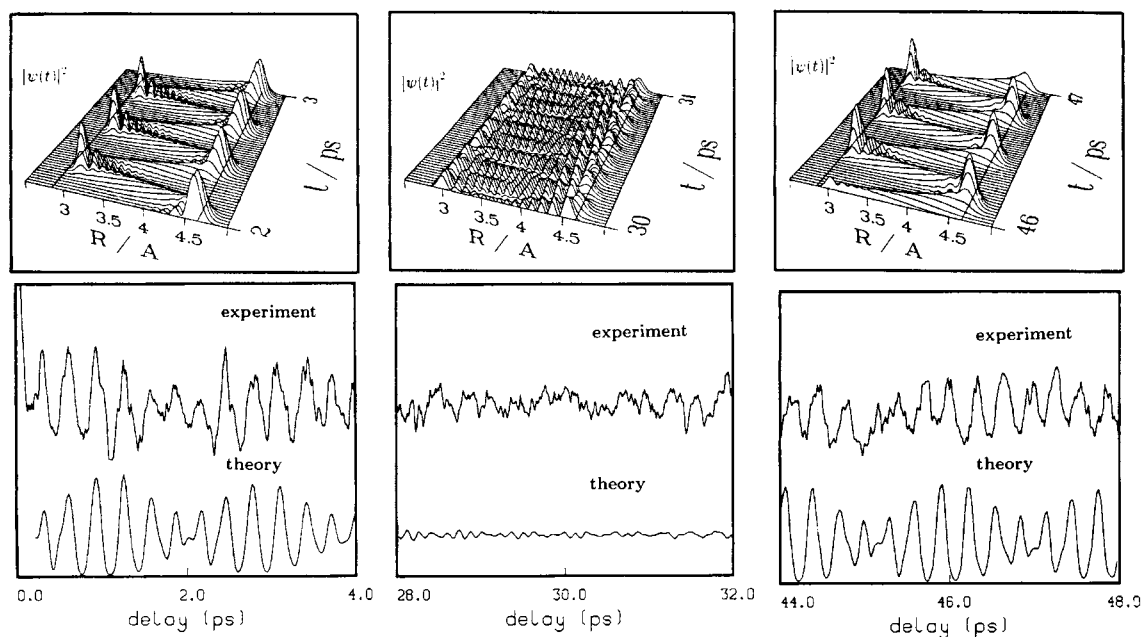
Fig.13. Snapshots of long-time behavior of the A $^1\Sigma_u^+$ state wave packet at three different times. The upper part shows in each case the dynamics of this vibrational wave packet. The straight lines parallel to the time axis indicate the classical turning points corresponding to the average energy of the packet. In the lower parts, the measured pump-probe ionization signal is shown as a function of delay time between the laser pulses and compared to the calculated total ionic population. *Left*: initial dynamics of the wave packet after 2 ps; *middle*: spreading of the wave packet after 30 ps; *right*: complete recurrence of the wave packet at 47 ps.
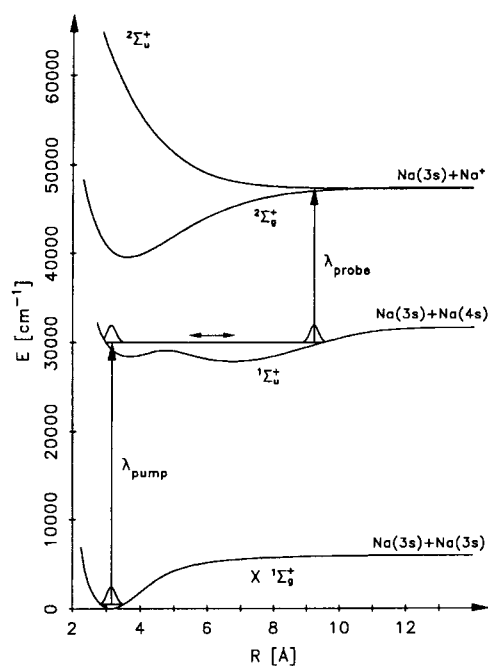

Fig.14. Potential energy diagram illustrating the basic idea of the double minimum experiment. The pump pulse creates a wave packet at the inner turning point of the potential. The probe laser is tuned such that the wavepacket is transferred only at the outer turning point onto the $^2\Sigma_u^+$ repulsive ionic curve.
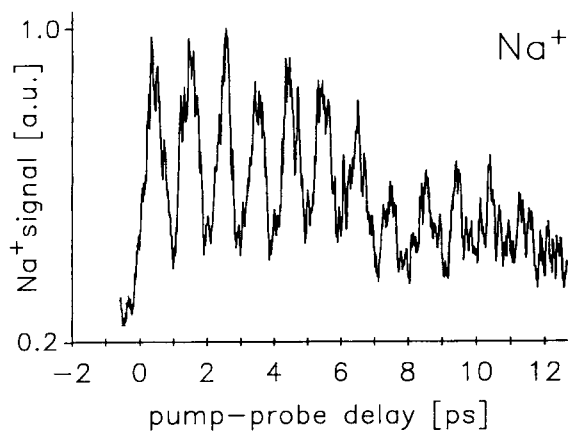

Fig.15. The Na^+ transient as a function of pump-probe delay shows an oscillation period of about 1 ps. This is the oscillation period of the $2\,^1\Sigma_u^+$ double minimum state of Na_2 at an excitation wavelength of 341 nm.

first experimental results are displayed. The Na^+ signal as a function of pump-probe delay time shows an oscillation period of 1 ps, in agreement with high-resolution spectroscopy. As the probe laser power dependence showed the onset of multiphoton behavior, the process displayed in Fig. 14 is probably not the only one responsible for the observed transient Na^+ signal. A multiphoton transition

Baumert and Gerber / Femtosecond Dynamics of Molecules

could be reasoned by a change of character of the electronic wave function in this double-minimum state along the internuclear axis. The state is formed by the avoided crossing of two adiabatic potential curves. The first of these is a Rydberg state, and the second has substantial ionic character at large internuclear distances.[26a,b] The experiment implies that ionization from the ionic character (Na^+ - Na^- like) into the $Na(3s)$ + Na^+ + e^- continuum is one mechanism, and the excitation into higher-lying doubly-excited electronic states of unknown character would be another possible mechanism. Our current experiments focus on other detection channels, and also on tuning the probe wavelength and measuring the emitted electrons in order to improve the overall temporal resolution and eventually measure the "fractional revivals".

F) Na_3 — Trimer

Femtosecond pump-probe techniques have also been employed to study the ionization and fragmentation dynamics of Na_3.[27] In the case of the B-state, an ultrashort 60 fs pump pulse with photons of 623 nm excites a coherent superposition of the lowest vibrational and pseudoro-tational levels, due to its bandwidth of about 300 cm^{-1}. The generated vibrational and pseudorotational wave packets propagate in the excited state potential surfaces. A time-delayed probe photon of the same wavelength and the same 60 fs time duration probes the motion of the wave packet and the decay of the excited state population. This is done by time-delayed probe photon ionization. The transient ionization spectrum of Na_3 obtained for a central wavelength of 623 nm is shown in Fig. 16. This time domain spectrum is more complex than that observed for the dimer Na_2. But there are still distinct recognizable time patterns, like the 320 fs separation of the major peaks, which correspond to an energy differ-
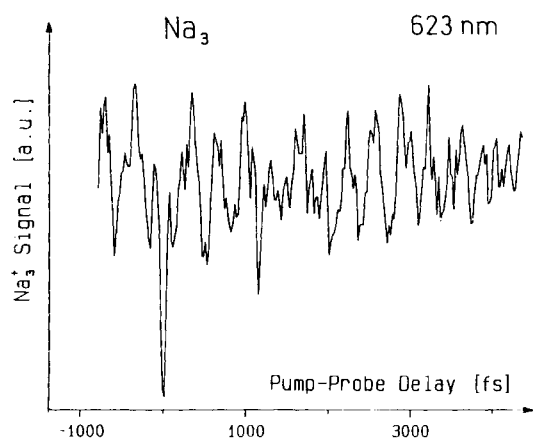
ence of 105 cm^{-1}, and the dip around zero time delay caused by fragmentation of the formed Na_3^+ by the intense laser fields at $\Delta t = 0$. It is in agreement with earlier high-resolution two-photon ionization (via B-state) spectra[28] that we do not observe a decay of the B-state for longer delay times up to 10 ps. As the fast Fourier transformation (FFT) spectrum, displayed in Fig. 17, shows, the dynamics of the two-photon ionization process is determined by three-dimensional wave packet motions in the Na_3 B-state and in the X-state as well. At the applied laser intensity, both states are involved. The pump laser generates a wave packet in the intermediate B-state and, simultaneously, a wave packet in the X electronic ground state through stimulated emission pumping during the pump pulse.

The contributions in the FFT spectrum (Fig. 17) near 140 cm^{-1}, 90 cm^{-1}, and 50 cm^{-1} are attributed to the symmetric stretch, to the asymmetric stretch, and to the bending mode in the Na_3 electronic ground state. This assignment is based upon the analysis of Broyer et al.[29] The wave packet dynamics in the excited B-state seems to be dominated by the symmetric stretch mode with frequencies close to 105 cm^{-1}. According to calculations of Meyer[30] and Cocchini et al.,[31] the eigenfrequencies of the symmetric stretch modes of the 4 $^2A_1$- and the 3 $^2B_2$- states are in the range of 94–111 cm^{-1}. The contribution around 72 cm^{-1} is tentatively assigned to the bending and asymmetric stretch mode of the 3 $^2B_2$-state.

The other observed frequencies, 8.5–12 cm^{-1}, 17.5–20 cm^{-1}, and 30.5–35 cm^{-1}, are assigned to a free pseudorotational wave packet motion in the potential surface of the B-state. The energy differences of successive pseudorotational j-states are experimentally determined and assigned by Delacretaz et al.[28] on the basis of a pure Jahn–Teller distortion of the B-state to half-integer

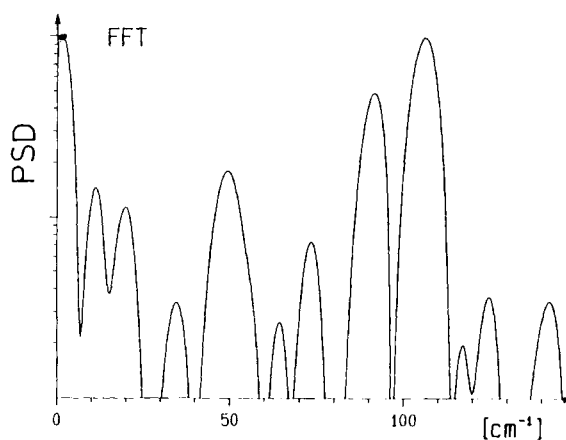Fig. 16. Pump-probe ionization spectrum of Na_3 (X- and B-states) using 60 fs light pulses at 623 nm.

Fig. 17. Fast Fourier transform spectrum of the Na_3 transient ionization spectrum shown in Fig. 16.

j-values. For $v = 0$, ($v = 1$), these values are Δ_j: 1/2, -3/2 = 2.5; (5) cm^{-1}, Δ_j: -3/2, 3/2 = 12; (13.5) cm^{-1}, Δ_j: 3/2, 5/2 = 18; (20) cm^{-1}, Δ_j: 7/2, 9/2 = 34; (30) cm^{-1}, respectively. It is, however, very interesting to note that in our experiment the corresponding radial component (128 cm^{-1}) of the pseudorotational motion only plays a minor role, if at all. In contrast to this, high-resolution spectroscopy of the B–X system exhibits a strong contribution of the radial pseudorotational component.[28] The reason for this difference is not yet fully understood (one possibility is due to the fact that the employed spectral width of the pump pulse centered around 623 nm barely couples the radial vibronic levels $v = 0$ and $v = 1$). Theoretical studies of Meiswinkel and Köppel[32] showed that the observed high-resolution spectra can also be explained by taking into account a pseudo-Jahn–Teller (PJT) model with integer pseudorotational j-values. In that model, the vibronic coupling of the accidentally degenerate (D_{3h}) states 3 $^2E'$ (B) and 2 $^2A'_1$ is responsible for the observed vibronic structure. So far, it is not yet clear which of the two models more appropriately explains the observed pseudorotational wave packet motion, since the ultrashort dynamics depends on the pseudorotational energy *differences*.

In an additional real-time experiment (see also ref 27) we measured the two-photon ionization-induced zero kinetic energy (ZEKE) photoelectrons[33] as a function of pump-probe delay time, using 60 fs light pulses at a wavelength of 618 nm. The fast Fourier transformation of the transient ZEKE electrons again showed the frequencies supporting vibrational wave packet motion in the X- and B-states and the pseudorotational wave packet motion in the B-state. In this experiment, the peak around 128 cm^{-1}, probably due to the B-state radial vibrational motion, is now clearly seen in contrast to the Na$_3^+$ Fourier transform spectrum. These differences are probably due to the different photon energies (618 nm vs. 623 nm) and the different ionization processes (direct photoionization vs. field-ionization of high-lying Rydberg states).

IV. SUMMARY

The real-time dynamics of multiphoton ionization and fragmentation of sodium molecules have been studied in molecular beam experiments employing femtosecond pump-probe techniques and ion and electron spectroscopy. Sodium with one valence electron per atom is experimentally and theoretically a very attractive system. Femtosecond time-resolved multiphoton ionization of sodium molecules reveals unexpected features in the dynamics of the absorption of several photons:

In Na$_2$, a second major REMPI process involving stepwise excitation of *two* electrons and subsequent electronic autoionization is observed, in addition to the direct

one electron photoionization process.

The femtosecond pump-probe technique demonstrates the possibility of controlling reactions by controlling the duration of propagation of a wave packet on an excited electronic surface, as the ratio of Na$_2^+$ vs. Na$^+$ varies by more than 100 % as a function of pump-probe delay time.

The contribution of the one-electron REMPI process versus the two-electron REMPI process to the total ion yield varies strongly with the applied laser field strength. This can be explained by coherent coupling of the electronic states participating in these REMPI processes, leading to laser intensity-dependent populations in these states. At high laser intensities a wave packet in the electronic ground state is observed, created by stimulated emission pumping during the pump pulse duration.

The 4 $^1\Sigma_g^+$ shelf state of Na$_2$ is given as an example of how to perform frequency spectroscopy of high-lying electronic states through time domain measurements.

The spreading and recurrence of a one-dimensional vibrational wave packet is described and compared to quantum calculations.

The three-dimensional wave packet motions on the bound potential energy surfaces of the X- and B-states of Na$_3$ are studied. The dynamics is determined by the normal modes of this trimer, and also shows the pseudorotational motion in the B state.

These real-time studies of the dynamics of ionization and fragmentation with femtosecond time resolution open up new and very exciting fields in molecular physics and yield results which, in many cases, are not accessible in nanosecond or picosecond laser experiments.

REFERENCES

(1) Baumert, T.; Bühler, B.; Thalweiser, R.; Gerber, G. *Phys. Rev. Lett.* 1990, **64**: 733.
(2) Baumert, T.; Röttgermann, C.; Rothenfußer, C.; Thalweiser, R.; Weiss, V.; Gerber, G. *Phys. Rev. Lett.* 1992, **69**: 1512.
(3) (a) Keller, J.; Weiner, J. *Phys. Rev. A* 1984, **30**: 213. (b) Burkhardt, C.E.; Barver, W.P.; Leventhal, J.J. *Phys. Rev. A* 1985, **3.31**: 505.
(4) Broyer, M.; Delacretaz, G.; Labastie, P.; Whetten, R.L.; Wolf, J.P.; Wöste, L. *Z. Phys. D* 1986, **3**: 131.
(5) Khundkar, L.; Zewail, A.H. *Annu. Rev. Phys. Chem.* 1990, **41**: 15 and references therein.
(6) Martin, J.L.; Migus, A.; Mourou, G.A.; Zewail, A.H., Eds.; *Ultrafast Phenomena VIII;* Springer Series in

114

Chemical Physics Vol. 55, Springer Verlag: Berlin, 1993.

(7) (a) Liu, Q.; Wang, J.K.; Zewail, A.H. *Nature* 1993, **364**: 427. (b) Papanikolas, J.M.; Vorsa, V.; Nadal, M.E.; Campagnola, P.J.; Gord, J.R.; Lineberger, W.C. *J. Chem. Phys.* 1992, **97**: 7002. (c) Baumert, T.; Thalweiser, R.; Weiss, V.; Gerber, G. *Z. Phys. D* 1993, **26**: 131. (d) Rothenfußer, C.; Thalweiser, R.; Weiss, V.; Gerber, G. *Phys. Rev. Lett.* Submitted.

(8) Baumert, T.; Grosser, M.; Thalweiser, R.; Gerber, G. *Phys. Rev. Lett.* 1991, **67**: 3753.

(9) Meyer, W. Private communication.

(10) Baumert, T.; Bühler, B.; Grosser, M.; Thalweiser, R.; Weiss, V.; Wiedenmann, E.; Gerber, G. *J. Phys. Chem.* 1991, **95**: 8103.

(11) Engel, V.; Baumert, T.; Meier, Ch.; Gerber, G. *Z. Phys. D* 1993, **28**: 37.

(12) Warren, W.S.; Rabitz, H.; Dahleh, M. *Science* 1993, **259**: 1581.

(13) Tannor, D.J.; Kosloff, R.; Rice, S.A. *J. Chem. Phys.* 1986, **85**: 5805.

(14) Potter, E.D.; Herek, J.L.; Pedersen, S.; Liu, Q.; Zewail, A.H. *Nature* 1992, **355**: 66.

(15) Baumert, T.; Engel, V.; Meier, C.; Gerber, G. *Chem. Phys. Lett.* 1992, **200**: 488.

(16) Meier, C. *Diplomarbeit Universität Freiburg* 1992, and private communication.

(17) Gruebele, M.; Roberts, G.; Dantus, M.; Bowman, R.M.; Zewail, A.H. *Chem. Phys. Lett.* 1990, **166**: 459.

(18) Janssen, M.H.M.; Bowman, R.M.; Zewail, A.H. *Chem. Phys. Lett.* 1990, **172**: 99.

(19) Wang, H.; Whang, T.J.; Lyyra, A.M.; Li, L.; Stwalley, W.C. *J. Chem. Phys.* 1991, **94**: 4756.

(20) Engel, V. *Chem. Phys. Lett.* 1991, **178**: 130, and private communication.

(21) Baumert, T.; Engel, V.; Röttgermann, C.; Strunz, W.T.; Gerber, G. *Chem. Phys. Lett.* 1992, **191**: 639.

(22) Averbukh, I.Sh.; Perelman, N.F. *Phys. Lett. A* 1989, **139**: 449.

(23) Gerber, G.; Möller, R. *Chem. Phys. Lett.* 1985, **113**: 546.

(24) (a) Alber, G.; Ritsch, H.; Zoller, P. *Phys. Rev. A* 1986, **34**: 1058. (b) Yeazell, J.A.; Mallalieu, M.; Stroud, C.R. *Phys. Rev. Lett.* 1990, **64**: 2007.

(25) Noordam, L.D. Private communication.

(26) (a) Cooper, D.L.; Barrow, R.F.; Verges, J.; Effantin, C.; d' Incan, J. *Can. J. Phys.* 1984, **63**: 1543. (b) Verges, J.; Effantin, C.; d' Incan, J.; Cooper, D.L.; Barrow, R.F. *Phys. Rev. Lett.* 1984, **53**: 46. (c) Delacretaz, G.; Wöste, L. *Chem. Phys. Lett.* 1985, **120**: 342. (d) Haugstätter, R.; Goerke, A.; Hertel, I.V. *Z. Phys. D* 1988, **9**: 153.

(27) Baumert, T.; Thalweiser, R.; Gerber, G. *Chem. Phys. Lett.* 1993, **209**: 29. Thalweiser, R.; Vogler, S.; Gerber, G. *SPIE Proc.* 1993, **1858**: 196.

(28) (a) Delacretaz, G.; Grant, E.R.; Whetten, R.L.; Wöste, L.; Zwanziger, J.F. *Phys. Rev. Lett.* 1986, **56**: 2598. (b) Rakowsky, S.; Herrmann, F.W.; Ernst, W.E. *Z. Phys. D* 1993, **26**:

(29) Broyer, M.; Delacretaz, G.; Ni, G.Q.; Whetten, R.L.; Wolf, J.P.; Wöste, L. *Phys. Rev. Lett.* 1989, **62**: 2100.

(30) Meyer, W. Private communication.

(31) Cocchini, F.; Upton, T.H.; Andreoni, W. *J. Chem. Phys.* 1988, **88**: 6068.

(32) Meiswinkel, R.; Köppel, H. *Chem. Phys. Lett.* 1990, **144**: 117.

(33) Müller-Dethlefs, K.; Sander, M.; Schlag, E.W. *Z. Naturforsch.* 1984, **39a**: 1089.